Journal of Applied Polymer Science

Effects of Dihydrogen Phosphate Intercalated Layered Double Hydroxides on the Crystal Behaviors and Flammability of Polypropylene

Xishan Liu, Xiaoyu Gu, Sheng Zhang, Yu Jiang, Jun Sun, Mingzhe Dong
Key Laboratory of Carbon Fiber and Functional Polymers, Ministry of Education, Beijing University of Chemical Technology, Beijing 100029, China
Correspondence to: X. Gu (E - mail: guxy@mail.buct.edu.cn)

ABSTRACT: Mg-Al-$H_2PO_4^-$ layered double hydroxides (LDHs) was prepared by anion exchange method, and polypropylene (PP)-LDH composites were prepared by melt compounding. The dispersion of LDH in PP matrix was characterized by Transmission electron microscope and X-ray diffraction (XRD), and the results showed that both exfoliation structures and aggregation structures can be found in the composites. The effects of LDH on the crystal behaviors of PP was investigated by XRD and Differential scanning calorimetry (DSC), and it indicated that LDH can induce the formation of β crystal and serve as a heterogeneous nucleating agent in PP. The significant decrease of both the crystallization and the melting enthalpy (ΔH_c and ΔH_m) was observed in PP composite at the presence of LDH platelets. Both the peak heat release rate and total heat release (THR) were significantly decreased after the addition of treated LDH. The possible chemical structural change in the condensed phase of PP composite during heating was studied by Fourier transform infrared spectroscopy (FT-IR). The mechanism of modified LDH in improving the fire performance of PP and the possible relationship between flame retardancy and crystal behavior have been proposed and discussed. © 2013 Wiley Periodicals, Inc. J. Appl. Polym. Sci. 130: 3645–3651, 2013

KEYWORDS: flame retardance; crystallization; thermogravimetric analysis

Received 4 April 2013; accepted 3 June 2013; Published online 26 June 2013
DOI: 10.1002/app.39614

INTRODUCTION

Polypropylene (PP) is one of the widely used polyolefins, whose application, however, is limited because of the poor fire behavior.[1,2] Polymer-clays nanocomposites have attracted significant interests during last decades owing to their remarkable improvements in physicochemical properties, especially thermal stability, reduced gas permeability and flammability.[3] It has been proved that the addition of montmorillonite (MMT), a layered silicate, into PP matrix can to some extent improve the flame retardancy.[4–7] However, another kind of anionic clay, layered double hydroxides (LDHs), the lamellar structure of which is similar to that of MMT has drawn enormous attention in recent years.[8–11]

It has been demonstrated that[12] thermal stability is improved in polymer-clays composites, because polymer chains are confined in a brucite-like layers, which reduces of the volatile production under high temperature from polymer matrix and slows air/oxygen transfer rate, leading to the increasing of its thermal decomposition temperature.

The general molecular formula of LDH is $[M^{2+}_{1-x}M^{3+}_x(OH)_2]^{x+}A^{n-}_{x/m}\cdot nH_2O$, where M^{2+} is divalent metallic cations, such as Mg^{2+}, Zn^{2+}, Cu^{2+}, Ni^{2+}, and M^{3+} is trivalent metallic cations, such as Al^{3+}, Co^{3+}, Mn^{3+}, Fe^{3+}, Ni^{3+}, while A^{n-} is interlayer anion, which is exchangeable and makes it possible to insert various anions into interlayer of hydrotalcite, such as CO_3^{2-}, NO_3^-, PO_4^{3-}, $H_2PO_4^-$ and so on, nH_2O is interlayer hydrone. Among the family of LDH, the hydrotalcite with Mg^{2+} and Al^{3+} anions and carbonate interlayer anions MgAl-CO_3 possesses the similar composition and structure to that of conventional flame retardants magnesium hydroxide (MH) and aluminium hydroxide (ATH).

In general, phosphorus-containing compounds are often used alone or combined with other flame retardants, which can increase the char amount and char efficiency of polymers during burning. These kinds of charred layers can decrease the amount of flammable volatile gases and reduce the heat transfer. Therefore, phosphorus-containing compounds intercalated LDH cannot only improve the dispersibility of LDH, but also enhance the fire performance of the composite.[13,14]

In our work, LDH was selected as a flame retardant, which had a double layered structure. $H_2PO_4^-$ was used to enlarge the basal spacing of LDH and as a phosphorus-containing flame retardant. Therefore, the polymer chains can easily enter the

interlamination of LDH to form a nano-dimension structure. If $H_2PO_4^-$ can exfoliate LDH particles in PP, the nano-dimension could provide stronger interactions and high interfacial strength between the dispersed LDHs particles and the polymers, which can improve the flammability and thermal stability of polymer in melt state.[15,16]

Therefore, the performance of LDH with phosphorus-containing compounds intercalated anion in the halogen-free flame retardant polymeric materials is an interesting topic.[17,18] As crystal behavior is closely related to polymer properties,[19] more work about the effects of MMT[20–23] on the crystal behavior of PP than that of LDH [24,25] has been reported. Previously we also reported that the LDH intercalated dihydrogen phosphate anion can enhance the fire performance of PP.[26]

This article reports the effects of LDH on both the crystal behavior and flammability of PP. The crystal behavior and the dispersion of treated LDH in PP are characterized. The possible relationship between flame retardancy and crystal behavior was analyzed. The flame retardant mechanism of H_2PO_4-LDH in PP composite was also proposed and discussed. To our best knowledge, this is the first time to correlates the crystal behavior and flammability in PP composite containing dihydrogen phosphate intercalated LDHs.

EXPERIMENTAL

Materials and Sample Preparation

PP (IPP/t30s) with a melt index of 3.0 g/10 min was purchased from Maoming Oil Company, China. Mg-Al-CO_3^{2-} LDH was purchased from Nantong Advance Chemicals, China. H_2PO_4-LDH was prepared in the lab.

1. Preparation of H_2PO_4-LDH

The dihydrogen phosphate-intercalated H_2PO_4-LDH was prepared by anion exchange method in aqueous solution. Briefly speaking, 13.6 g Mg-Al-CO_3^{2-} and 14 g NaH_2PO_4 was mixed and stirred vigorously in water at pH value of around 4.5 under flowing N_2 gas protection (30 mL/min). After aging in a mother liquid at 100°C for 2 hours, the precipitate was washed with distilled water in vacuum Buchner funnel until the PH value of filtrates is 7.0. Then the precipitate were dried in oven at 60°C for 24 h and yielded H_2PO_4-LDH.

2. Preparation of PP/LDH composites

The PP/LDH composite were melt compounded by a co-rotating two-screw extruder (SHL-35, 4th Shanghai Chemical Machinery Plant, China, L/D = 35, L = 0.88 m). The temperature setting of extruder from the hopper to the die was 180/190/195/200/200/190°C, and the screw speed was 50 rpm. The pelletized granules were dried for 6 hours under 80°C before injected to the suitable thickness and size for Limited oxygen index (LOI), UL-94 and CCT tests by an injection molder (JPH-120; Guangdong Only Machinery Co, China). The temperature setting of injection molder from the hopper to the spray nozzle was 180/190/195/200°C. The injection pressure was 25–50 MPa. The injection time was 15 s, and the cooling time was 20 s. The contents of LDHs in the recipes were weighted parts per 100 part PP.

Characterizations

Fourier transform infrared spectroscopy (FT-IR) spectra were collected from a Fourier transformation infrared spectrometer Nicolet Nexsus 670 under the resolution of 1 cm^{-1} in 128 scans, and the correlative powders were studied by using KBr pellets. X-ray diffraction (XRD) patterns were recorded by a D/max2500 VB2+/PC X-ray diffractometer. The CuKα radiation source was operated at 40 KV and 20 mA. The samples were filled into a quadrate hollow aluminum holder, and LDHs and M-LDHs were analyzed as powders. Samples of PP/LDHs and PP/M-LDHs were from the injection mold. Patterns were recorded by monitoring those diffractions that appears from 5 to 70°. The scan speed was 2°/min.

The crystallization behavior was described by a Differential scanning calorimetry (DSC) Perkin-Elmer Pyris1. Each sample (about 5 mg) was first heated to 180°C at a heating rate of 10°C/min, and then held at 180°C for 5 min to eliminate the thermal history. The non-isothermal crystallization behavior was recorded with the cooling curve from 180 to 40°C at a cooling rate of 10°C/min. The second heating curve was recorded at a heating rate of 10°C/min from 40 to 180°C, exhibiting the trace of melting process.

TGA was performed in a TAQ-5000 with a heating rate of 10°C/min at a temperature range of 50–800°C under nitrogen atmosphere with a flow rate of 50 mL/ min. And the mass of each sample is approximately 3–5 mg. LOI and UL-94 vertical burning test was conducted according to ISO1210:1992 standard. The dimensions of samples for LOI and UL-94 tests were 100 × 6.5 × 3 mm^3 and 125 × 12.5 × 3 mm^3, respectively.

Fire testing technology cone calorimeter was also used to evaluate the fire performance of the composite according to the standard ISO 5660 under a heat flux of 50 kW/m^2 with a size of 100 × 100 × 4 mm^3 which was comparable to that of a mild fire scenario. Specimens were wrapped in aluminum foil, leaving the upper surface exposed to the radiator, and then placed on ceramic backing board at a distance of 25 mm from cone base. The experiments were repeated five times. Various parameters are obtained, including the time required to ignition, heat release rate (HRR), peak heat release rate (PHRR), total heat released (THR).The morphological analysis was carried out using JAPAN JEM-3010 transmission electron microscopy (TEM) at ambient temperature, with 200 kV acceleration voltage and bright field illumination.

RESULTS AND DISCUSSION

Dispersion of H_2PO_4-LDH in PP Matrix

TEM microphotographs of PP/12 phrH_2PO_4-LDH at 20K times (a) and 50K times (b) are shown in Figure 1. The dispersion state of H_2PO_4-LDH in PP matrix can be observed clearly. The platelet-like LDH sheets are scattered homogenously in the PP matrix with a particle size of about 200 nm long.

The XRD patterns of PP, H_2PO_4-LDH and PP/12phr H_2PO_4-LDH shows that the diffraction peaks of PP at $2\theta \approx 14°$ (110),

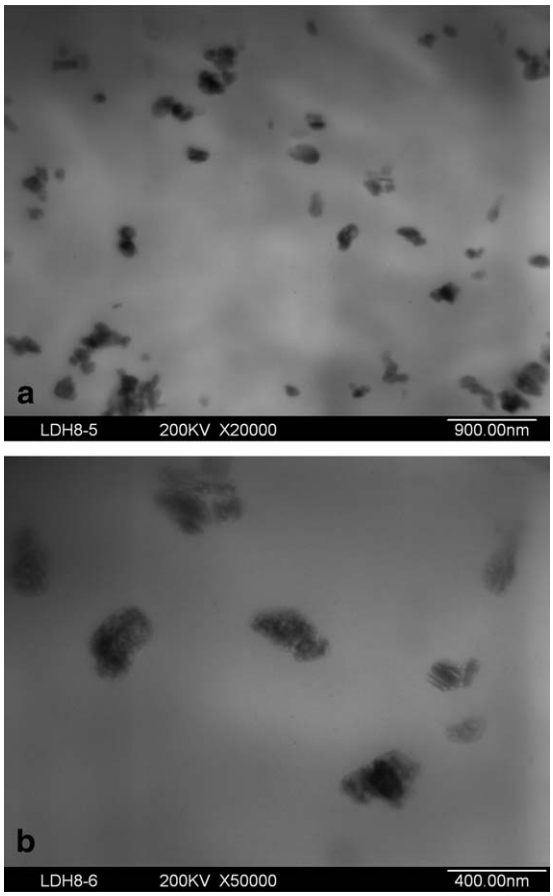

Figure 1. (a) TEM micrographs of PP/12 phr H_2PO_4-LDH nanocomposites at 20K times, (b) TEM micrographs of PP/12 phr H_2PO_4-LDH nanocomposites at 50K times.

16.6° (040), 18.3° (130), 21.1° (111), 21.7° (131), 25.1° (041) still exist in PP/H_2PO_4-LDH composite (Figure 2). And the diffraction peak at $2\theta = 7.3°$ for H_2PO_4-LDH could be found little in PP/H_2PO_4-LDH composite, The results maybe in part due to the damaged lamella structure of H_2PO_4-LDH and subsequently formation of exfoliated structure in PP matrix. One can also see that a new reflection peaks appears at $2\theta \approx 15.8°$, which will be discussed more in the next section below.

After the exchange of CO_3-LDH to H_2PO_4-LDH, the interlayer spacing was enlarged. As a result H_2PO_4-LDH became much easier to form the exfoliation structure than CO_3-LDH. But it is still difficult to achieve totally exfoliated structure without any compatibilizer. Finally both exfoliation and aggregation structure can be found in the composites in this work.

Crystal Behaviors

XRD. It has been reported that α crystal form in PP is corresponding to reflection peaks at $2\theta \approx 14°$ (110), 16.6° (040), 18.3° (130), 21.1° (111), 21.7° (131), 25.1° (041), and 28.3° (060), while β form is corresponding to that at $2\theta \approx 15.8°$ (020).[27] Only α crystal form of neat PP could be seen from XRD curves shown in Figure 3. However, both α [14° (110), 16.6° (040), 18.3° (130), 21.1° (111), 21.7° (131), 25.1° (041)) and β (15.8° (300)] could be observed in PP/H_2PO_4-LDH composite, which

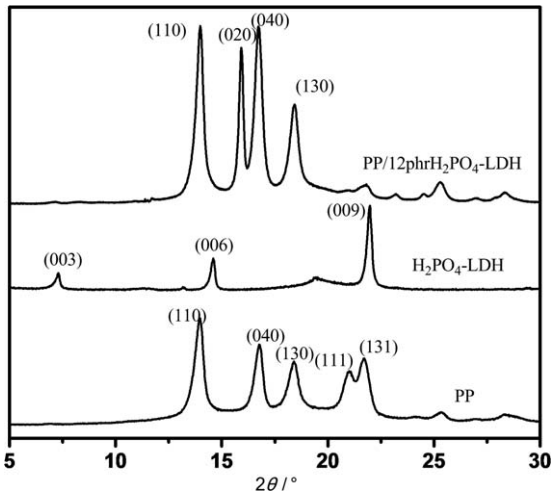

Figure 2. XRD patterns of PP, H_2PO_4-LDH and PP/12 phr H_2PO_4-LDH.

indicated the existing of H_2PO_4-LDH in PP matrix induces the formation of β form.

The crystallite size can be obtained by using the Derby–Scherrer expression:

$$\langle D \rangle = \frac{k\lambda}{\beta \cos\theta}$$

Where D is the crystallite size in the normal direction of the selected set of crystal planes, 2θ is the Bragg reflection angle of the corresponding set of crystal planes, k is the Derby–Scherrer constant ($k = 0.9$), λ is the X-ray wavelength ($\lambda = 0.154$nm for Cu-Kα radiation), β is the calibrated half-width of Bragg reflection peak [$\beta = (B^2 - b_0^2]^{1/2}$, B is the experimental half-width of the peak, and b_0 is the instrumental broadening factor, hereby b_0=0.16°. Apparently, D is inversely proportional to β when θ is given, and vice versa.[28]

The diffraction peak at $2\theta \approx 14°$ (Figure 3) is assigned to the Bragg reflections by α crystal plane of (110). Each set of crystal planes, according to Derby–Scherrer expression, corresponds to

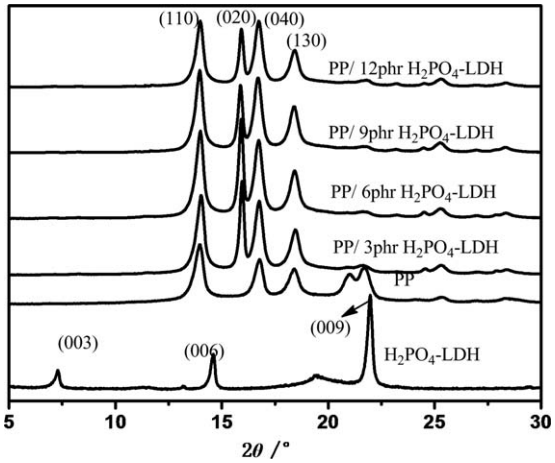

Figure 3. XRD patterns of H_2PO_4-LDH, PP and PP/ H_2PO_4-LDH nanocomposites

Table I. Crystallite Size Indicator at α (110) for PP and PP/LDH Nanocomposites

H_2PO_4-LDH content (phr)	110 (nm)	040 (nm)	130 (nm)
Neat PP	17.5	19.6	16.1
3	19.8	24.5	17.8
6	20.1	24.3	18.3
9	20.7	24.2	18.9
12	20.8	24.5	18.9

Table II. Parameters of PP/LDH Nanocomposites from DSC Curves

H_2PO_4-LDH content/phr	T_c (°C)	T_m (°C)	ΔT (°C)	ΔH_c (J/g)	ΔH_m (J/g)	Xc (%)
neat PP	119.9	164.4	44.5	98.3	107.7	47.5
3	121.5	162.4	40.9	94.9	98.9	45.8
6	121.6	163.7	42.1	94.4	97.1	45.6
9	121.9	163	41.1	89.5	95.2	43.2
12	122.1	162.4	40.3	85.0	90.0	41.1

their own Derby–Scherrer expression, in which β_{110} is inversely proportional to D_{110}. Therefore, its half-width β_{110} should basically have a negative correlation with crystallite size. If the left item D of Derby–Scherrer expression is defined as when β_{110} is taken as β in the right item, β_{110} also has a negative correlation with as shown by eq. (1). Thus should be a positive indicator (Table I) for crystallite size. Addition of H_2PO_4-LDH can significantly increase the crystallite size indicator , however the increases of with the content of H_2PO_4-LDH from 3 to 12 phr is minimal (Table I), indicating crystallite size was progressively promoted by the dispersed H_2PO_4-LDH in PP matrix.

DSC. The crystallization and melting behaviors of PP composites were analyzed by DSC. Figure 4 presents the cooling DSC traces after eliminating thermal-history, and Table II provides some key thermal data obtained from DSC curves.

Figure 4 shows crystallization temperature (T_c) in the cooling process increases from 119.9 to 121.5, 121.6, 121.9, and 122.1°C for samples with LDH content varying from 0, to 3, 6, 9, and 12 phr. In other words, T_c shifts towards higher temperature with increasing LDH content. Meanwhile, the melting temperature (T_m) during the second heating process decreases a bit in PP/LDH composties compared with neat PP (Table II). As a result, the super-cooling temperature (ΔT), which is the difference between T_m and T_c ($\Delta T = T_m - T_c$) is decreasing, resulting in a larger nuclei size in PP/H_2PO_4-LDH composites than pure PP.

It can be seen from Table II that the crystallization enthalpy (ΔH_c) decreases from 98.3 of neat PP to 94.9, 94.4 89.5, and 90 J/g of PP composite samples, which indicates LDH can lower the crystallinity of PP composite. The same tendency also applies to the second heating process, where ΔH_m decreases and T_m increases with LDH content. Together with the XRD analysis, scattered LDH lamellas did serve as a nucleation agent in PP matrix, leading to a higher beginning temperature for the crystallization process. On the other hand, the crystallinity of PP decreases with the content. The decrease in crystallinity induced by the LDH may be due to the restricted mobility of the PP molecular chains in the lamellas of LDH.

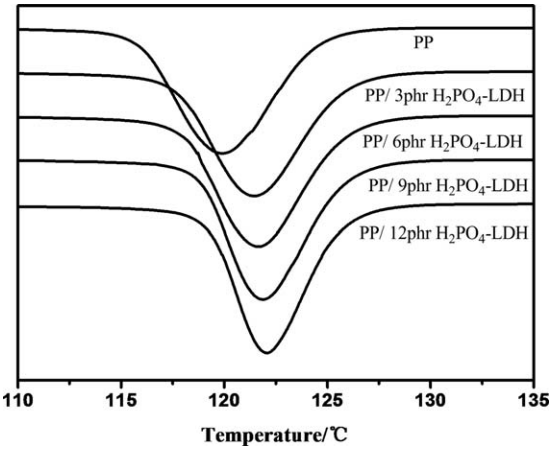

Figure 4. DSC curves of PP and PP/LDH nanocomposites at a cooling rate of 10°C/min.

Thermal Behavior Analysis

The thermal behaviors of H_2PO_4-LDH and its effects on thermal stability of the PP were studied by TGA (Figures 5 and 6). In order to compare the thermal stability of composites with different H_2PO_4-LDH loadings, several typical decomposition temperatures stemmed from curves in Figure 6 are summarized in Table III. It demonstrates the initial decomposition temperature ($T_{5\%}$) at which 5% weight loss takes place, the half decomposition temperature ($T_{50\%}$) at which 50% weight loss takes place and the maximum heat loss temperature (T_{endo}) at which the maximum weight loss rate happens.

The H_2PO_4-LDH undergoes four-stage decomposition process (Figure 5), of which the first two appears before 230°C with a weight loss of around 12%, due to the possible liberation of physical absorbed water and loss of hydroxide on LDH.[29] The third and fourth steps range from 230°C to 500°C with a weight loss <17%, which may be caused by the collapse of crystalline structure resulting from the dehydroxylation of the host

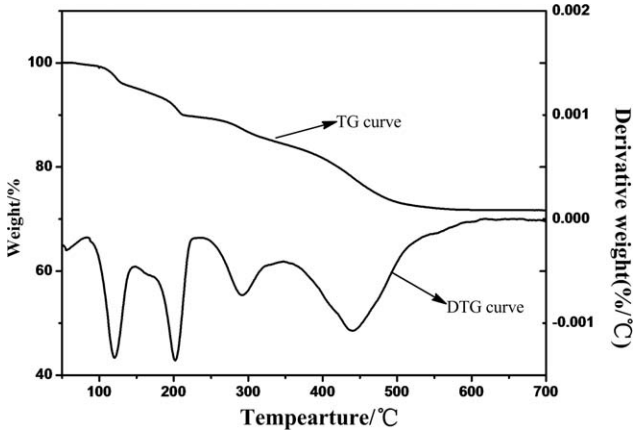

Figure 5. TG and DTG curves of H_2PO_4-LDH.

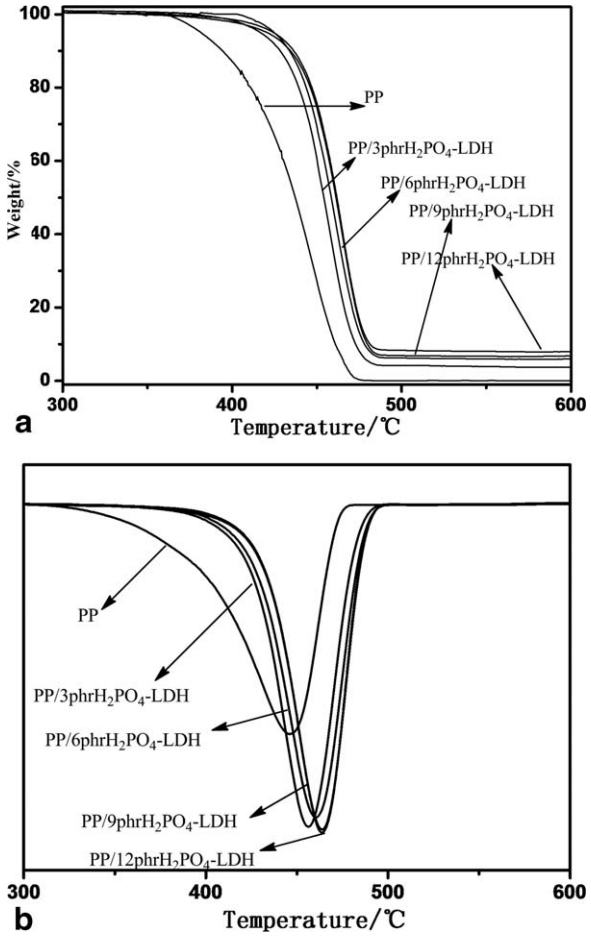

Figure 6. (a) TG curves of PP and PP/LDH nanocomposites, (b) DTG curves of PP and PP/LDH nanocomposites.

layers in H_2PO_4-LDH. The char residue at 800°C is around 70%.

It is suggested the dispersed clay sheet layers form a barrier effect during the PP/LDH composites decomposition under the high temperature, in which it is difficult for the inner volatile product to spread out and the outside air/oxygen to enter. The increase of thermal decomposition temperature of PP nanocomposite indicates that LDH can improve thermal stability of the materials.

According to Figure 6, both TG and DTG curves of PP/LDH composites obviously shift to a higher temperature compared to that of neat PP, and $T_{5\%}$, $T_{50\%}$, and T_{endo} values of PP

Table III. TG and DTG Data of PP and PP/ LDH Nanocomposites

H_2PO_4-LDHs content (phr)	$T_{5\%}$ (°C)	$T_{50\%}$ (°C)	Char (%)	T_{endo} (°C)
Neat PP	381.5	437	0	441
3	416.8	454.3	2.1	456.5
6	424.7	458.6	4.6	460.5
9	420.6	461.4	5.7	464
12	424.4	461.8	7.9	463.7

Table IV. LOI and UL-94 Results for PP and PP/LDH Nanocomposites

H_2PO_4-LDHs (phr)	LOI (%)	Time to dripping (s)	UL-94 rating
neat PP	17.8 ± 0.1	3 ± 1	No rating
3	18.4 ± 0.1	9 ± 1	No rating
6	18.8 ± 0.2	15 ± 1	No rating
9	19.5 ± 0.1	30 ± 1	No rating
12	21.2 ± 0.2	38 ± 2	No rating

composite increased as well. Anyway the release of water could also absorb heat and dilute the fuel concentration, which is also helpful in improving the fire performance. Interestingly, there is almost no residue left at 500°C for neat PP, while the char residue amount of composites is observably increased with the H_2PO_4-LDH loading. The char residue shown in Table III is about 70% of the H_2PO_4-LDH loaded PP. Considering the fact that H_2PO_4-LDH itself can leave 70% char at 800°C (Figure 5), it can be proposed that the presence of H_2PO_4-LDH cannot promote the char formation of PP substrate in this case. The char layer formed by the H_2PO_4-LDH could reduce the flammability of PP composite through coating mechanism in condensed phase, which blocks the air to underlying substrate and fuel to the flame zone. The amount of char residue in cone test is more or less similar to that in TGA test presented in Table IV.

The Flammability

The flammability of PP and its composites has been investigated by LOI, UL-94 tests and cone calorimeter test (Table IV).

LOI and UL-94 results demonstrate neat PP is very easy to burn with a lot of dripping. The LOI value for neat PP is only 17.8%, whereas increment can be seen in the composite containing LDH. The LOI value reaches 21.2% for the PP sample containing 12 phr H_2PO_4-LDH. Further improvement is also found in the UL94 vertical test results. The time required to start dripping from ignition directly influences the probability of escape and rescue during real fire hazard. Although all samples can be found dripping during burning, the time to start dripping is significantly prolonged after the addition of H_2PO_4-LDH. The time to dripping of sample with 12 phr H_2PO_4-LDH is 38 s which is almost 12 times longer than that of neat PP.

Cone calorimeter was also selected to evaluate the flammability of neat PP and its composites, for typical parameters derived from cone calorimeter test can be correlated to large-scale fire tests which are used to predict the flame hazards in real fire scenarios. The HRR curves and some combustion parameters obtained from cone calorimeter for pure PP and its nanocomposite-containing 12 phr LDH are shown in Figure 7 and Table V. The peak value of HRR (PHRR) decreases from 1302 kW/m^2 of neat PP to 534 kW/m^2 of PP/LDH composite, which means the presence of LDH can reduce 59% of PHRR value. The average HRR of the PP/LDH composite is 109 kW/m^2, which was 73.9% lower than that of the neat PP. The THR of the PP/LDH composite (62 MJ/m^2) was also 45.6% lower than that of the neat PP (114 MJ/m^2). These results show that

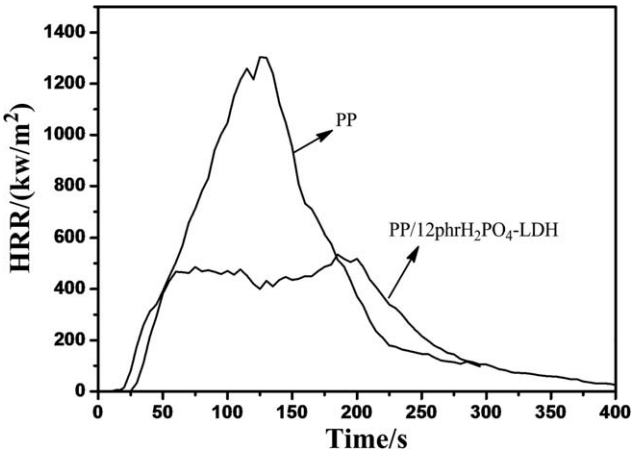

Figure 7. HRR curves of PP and PP/LDH nanocomposites.

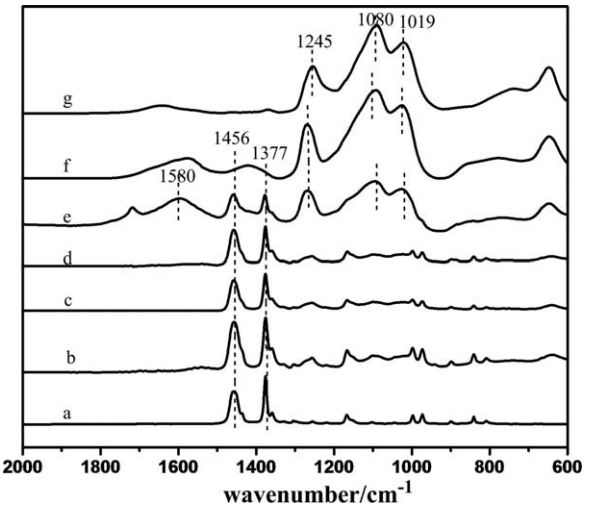

Figure 8. FTIR spectra of H_2PO_4-LDH and char residue of PP nanocomposite.(a) FT-IR spectrum of PP nanocomposite at 20°C. (b,c,d,e and f) FT-IR spectra of char residue of PP nanocomposite at 200, 250, 300, 350, and 400°C, respectively. (g) FT-IR spectrum of H_2PO_4-LDH.

the H_2PO_4-LDH had positive effects on improving the flame retardancy of PP. It also shows that the average mass loss rate (MLR, 0.0419 g/s) of the PP/LDH composite during combustion was lower than that of the neat PP sample (0.0519 g/s), which indicates that the MLRs of the samples were reduced after the adding of H_2PO_4-LDH.

Characterization of Char

FT-IR has been used to investigate chemical structures of the char residue. Figure 8 shows the FTIR spectra of PP/LDH composite char residue obtained under different temperature of 20, 200, 250, 300, 350, and 400°C (a–f). The two characteristic groups in PP are —CH_2— and —CH_3, whose asymmetric deformation vibrations are reflected in FT-IR at 1456 cm^{-1} and 1377 cm^{-1}. The two peaks have little change before 300°C [Figure 8(a–d)], while the strength of the peaks at both 1456 cm^{-1} and 1377 cm^{-1} at 350°C (e) is decreased dramatically, and almost disappear at 400°C (f) because of the rapid decomposition of PP during this period. New absorption peak at 1580 cm^{-1} appears when temperature is above 350°C, which is assigned to the C═C stretching vibration. It is suggested the formation of C═C double bonds could be due to the breakdown of PP main chains.

The absorption bands at 1245 cm^{-1} and 1080 cm^{-1} in the spectrum of H_2PO_4-LDH (g) are assigned to symmetric and asymmetric stretching vibration of the phosphorus oxygen double bond (P═O), respectively. The absorption band at 1019 cm^{-1} is assigned to the phosphate-carbon (P—C) vibration in complexes.[14,30] The strength of the three peaks is relatively weak at lower temperature because the low concentration of H_2PO_4-LDH in PP composite. However, the strength of the three peaks becomes intense when temperature is above 350°C (e,f) with the degradation of PP, which demonstrates most phosphorus compounds are remained in the char residue.

The FT-IR results further demonstrated that H_2PO_4-LDH will influence the degradation of PP at higher temperature range (above 350°C). The presence of P—O and P—C bonds in char layers after heating suggested that $H_2PO_4^-$ mainly take effect in the condensed phase through improving the char quality, the charred layers could prevent air/oxygen and heat transmission to slow down the spread rate of fire.

The Flame Retardant Mechanism of H_2PO_4-LDH

The improvement of thermal stability and flame retardancy of PP composite endowed by the incorporation of H_2PO_4-LDH can be attributed to several factors. Similar to other polyolefin, the molecular chains of PP consist of carbon and hydrogen. The combustion of PP is a typical radical chain reaction including chain initiator, propagation, and termination. Compared with PE, the hydrogen atom on the tertiary carbon exhibits higher reactive activity, which leads to lower thermal ability of PP. For a large amount of radicals are produced during chain initiator process of burning, the LOI value of PP is only 17–18%. As a crystal polymer, the arrangement of molecular chains are partly orderly and compact, as a result the rate of chain propagation is very fast and at the same time a large amount of droplets are generated during combustion. The PP is completely combusted without any char residue and shows high HHR.

It is reported[14] that free radicals of $PO^{\cdot}$, released by $H_2PO_4^{\bullet}$ during heating, could capture free radicals of $H^{\cdot}$ or $HO^{\cdot}$ which are produced during the initial degradation process. In other words, the H_2PO_4-LDH acts as a radical catcher to inhibit the degradation. It has been acknowledged that the reduction of

Table V. Some Key Combustion Parameters Obtained from Cone Calorimeter

H_2PO_4-LDHs (phr)	PHRR (kW/m²)	Average HRR (kW/m²)	THR (MJ/m²)	Average MLR (g/s)	Char residue (%)
neat PP	1302 ± 47	417 ± 24	114 ± 10	0.0519 ± 0.005	0 ± 0. 3
12	534 ± 18	109 ± 9	62 ± 5	0.0419 ± 0.003	8 ± 0.4

free radicals at the initial stage of fire is an effective way to improve the flame retardancy.

Besides, the flame retardation is contributed by the basic structure of LDH molecules, which is similar to MH and ATH, gives rise to an excellent physical barrier effect, particularly when the platelets exfoliated homogenously in the PP matrix. The delaminated state of the H_2PO_4-LDH in PP has also been evidenced by TEM and XRD results. Although the nano-dispersed LDH molecules acting as a nucleation agent can make the crystallization earlier, sheet-like dispersion among flexible PP molecular chains also limits its movement, which results in the decrease of crystallinity of PP. On the other hand, for the molecular chains of PP are confined in the barriers formed by the sheet-like LDH molecules, the reaction rate during combustion is suppressed, leading to the significant prolongation of the time to start dripping, therefore a better flame retardant performance and thermal stability was achieved.

Furthermore, the release of the constituent water from LDH can dilute the flammable gases produced by the degradation of PP during heating and absorbing heat, which can suppress the initial decomposition of polymer matrix.

CONCLUSIONS

Dihydrogen phosphate intercalated LDHs and PP/LDH composites were successful prepared. β form crystal can be formed and the crystallite size is increased in PP in the presence of H_2PO_4-LDH. The heterogeneous nucleation and the larger nuclei size induced by the presence of H_2PO_4-LDH in PP have been suggested to be closely related to both the thermal behavior and fire performance of PP. The improvement on thermal stability and flame retardation is attributed to the special structure of H_2PO_4-LDH and its dispersion status in PP. It is suggested that the modified LDH could affect the thermal stability through changing the crystal behavior.

It has been proposed that the flammability reduction of PP/H_2PO_4-LDH composite could be mainly due to the free radical capture of $PO^{\cdot}$, the barriers formed by the sheet-like LDH molecules which can restrict the motion of polymer chains, the decrease of crystallinity of PP, and the release of the constituent water from LDH which can dilute the flammable gases and absorb heat during combustion.

ACKNOWOLEDGMENTS

The authors would like to thank the National Natural Science Foundation of China (No. 21061130552/B040607) and the Fundamental Research Funds for the Central University China (ZZ1119) for their financial support.

REFERENCES

1. Zhang, S.; Horrocks, A. R. *Prog. Polym. Sci.* **2003**, *28*, 1517.
2. Wen, X.; Wang, Y. J.; Gong, J.; Tang, T. *Polym. Degrad. Stabil.* **2012**, *97*, 793.
3. Kumar, A. P.; Depan, D.; Tomer, N. S.; Singh, R. P. *Prog. Polym. Sci.* **2009**, *34*, 479.
4. Alberto, F.; Fibio, C.; Giovanni, C. *Polym. Degrad. Stabil.* **2012**, *98*, 2619.
5. Szustakiewicz, K.; Kiersnowski, A.; Gazinska, M. *Polym. Degrad. Stabil.* **2011**, *96*, 291.
6. Qin, H. L.; Zhang S. M.; Zhao, C. G. *Polym. Degrad. Stabil.* **2004**, *85*, 807.
7. Chen, X. S.; Yu, Z. Z.; Liu, W.; Zhang, S. *Polym. Degrad. Stabil.* **2009**, *94*, 1520.
8. Kuila, T.; Srivastava, S. K.; Bhowmick, A. K. *Compos. Sci. Technol.* **2008**, *68*, 3234.
9. Ardanuy, M.; Velasco, J. I. *Appl. Clay. Sci.* **2011**, *51*, 341.
10. Wang, D. Y.; Das, A.; Leuteritz, A.; Heinrich, G. *Polym. Degrad. Stabil.* **2011**, *96*, 285.
11. Du, B. X.; Guo, Z. H.; Fang, Z. P. *Polym. Degrad. Stabil.* **2009**, *94*, 1979.
12. Vaccari, A. *Appl. Clay. Sci.* **1999**, *14*, 161.
13. Li, N.; Xia, Y.; Mao, Z. W.; Wang, L.; Zheng, A. N. *Polym. Degrad. Stabil.* **2012**, *97*, 1737.
14. Ye, L.; Qu, B. J. *Polym. Degrad. Stabil.* **2008**, *93*, 918.
15. Ray, S.; Okamoto, M. *Prog. Polym. Sci.* **2003**, *28*, 1539.
16. Kumar, A. P.; Depan, D.; Tomer, N. S.; Singh, R. P. *Prog. Polym. Sci.* **2009**, *34*, 479.
17. Woo, M. A.; Kim, T. W.; Paek M. J.; Ha, H. W.; Choy, J. H. Hwang, S. J. *J. Solid. State. Chem.* **2011**, *184*, 171.
18. Castantino, U.; Casciola, M.; Massinelli, L.; Nocchetti, M.; Vivani, R. *Solid State Ionics* **1997**, *97*, 203.
19. Suprakas, S. R.; Masami, O. *Prog. Polym. Sci.* **2003**, *28*, 1539.
20. Zhu, S. P.; Chen, J. Y.; Zuo, Y; Li, H. L; Cao, Y. *Appl. Clay. Sci.* **2011**, *52*, 171.
21. Rozanski, A.; Monasse, B.; Piorkowska, E. *Eur. Polym. J.* **2009**, *45*, 88.
22. Ding, C.; Jia, D. M.; He, H.; Guo, B. C.; Hong, H. Q. *Polym. Test.* **2005**, *24*, 94.
23. Ray, V. V.; Banthia, A. K.; Schick, C. *Polymer* **2007**, *48*, 2404.
24. Ardanuy, M.; Velasco, J. I.; Realinho, V. *Thermochim. Acta.* **2008**, *479*, 45.
25. Lonkar, S. P.; Morlat, T. S.; Singh, R. P. *Polymer* **2009**, *50*, 1505.
26. Liu, X. S.; Gu, X. Y.; Jiang, Y.; Zhao, B.; Zhang, S. 2nd International Symposium on Flame-Retardant Materials & Technologies, Chengdu, China, September17–20, **2012**.
27. Canetti, M; Scafati, S. T. *Polym. Degrad. Stabil.* **2012**, *97*, 81.
28. Li, Y. Y.; Li, C. Y, Ni, C. Y.; Rong, L. X.; Hsiao, B. *Polymer* **2007**, *48*, 3452.
29. Wilkie, C. A.; Nyambo C. *Polym. Degrad. Stabil.* **2009**, *94*, 506.
30. Nyambo, C.; Kandare, E.; Wilkie, C. A. *Polym. Degrad. Stab.* **2009**, *94*, 513.